



CHORUS

This is the accepted manuscript made available via CHORUS. The article has been published as:

^{139}La NMR investigation of the charge and spin order in a $\text{La}_{1.885}\text{Sr}_{0.115}\text{CuO}_4$ single crystal

A. Arsenault, S. K. Takahashi, T. Imai, W. He, Y. S. Lee, and M. Fujita

Phys. Rev. B **97**, 064511 — Published 14 February 2018

DOI: [10.1103/PhysRevB.97.064511](https://doi.org/10.1103/PhysRevB.97.064511)

^{139}La NMR investigation of charge and spin order in $\text{La}_{1.885}\text{Sr}_{0.115}\text{CuO}_4$ single crystal

A. Arsenault and S. K. Takahashi

Department of Physics and Astronomy, McMaster University, Hamilton, Ontario L8S4M1, Canada

T. Imai

*Department of Physics and Astronomy, McMaster University, Hamilton, Ontario L8S4M1, Canada and
Canadian Institute for Advanced Research, Toronto, Ontario M5G1Z8, Canada*

W. He and Y. S. Lee

*Stanford Institute for Materials and Energy Sciences,
Stanford National Accelerator Laboratory, Menlo Park, CA 94025 and
Department of Applied Physics, Stanford University, Stanford, CA 94305*

M. Fujita

Institute for Materials Research, Tohoku University, Sendai 980-8577, Japan

(Dated: January 16, 2018)

^{139}La NMR is suited for investigations into magnetic properties of La_2CuO_4 -based cuprates in the vicinity of their magnetic instabilities, owing to the modest hyperfine interactions between ^{139}La nuclear spins and Cu electron spins. We report comprehensive ^{139}La NMR measurements on a single crystal sample of high T_c superconductor $\text{La}_{1.885}\text{Sr}_{0.115}\text{CuO}_4$ in a broad temperature range across the charge and spin order transitions ($T_{\text{charge}} \simeq 80$ K, $T_{\text{spin}}^{\text{neutron}} \simeq T_c = 30$ K). From the high precision measurements of the linewidth for the nuclear spin $I_z = +1/2$ to $-1/2$ central transition, we show that paramagnetic line broadening sets in precisely at T_{charge} due to enhanced spin correlations within the CuO_2 planes. Additional paramagnetic line broadening ensues below ~ 35 K, signaling that Cu spins in some segments of CuO_2 planes are on the verge of three dimensional magnetic order. A static hyperfine magnetic field arising from ordered Cu moments along the ab-plane, however, begins to develop only below $T_{\text{spin}}^{\mu\text{SR}} = 15 \sim 20$ K, where earlier μSR measurements detected Larmor precession for a small volume fraction ($\sim 20\%$) of the sample. Based on the measurement of ^{139}La nuclear spin-lattice relaxation rate $1/T_1$, we also show that charge order triggers enhancement of low frequency Cu spin fluctuations inhomogeneously; a growing fraction of ^{139}La sites is affected by enhanced low frequency spin fluctuations toward the eventual magnetic order, whereas a diminishing fraction continues to exhibit a behavior analogous to the optimally superconducting phase even below T_{charge} . These ^{139}La NMR results corroborate with our recent ^{63}Cu NMR observation that a new type of very broad, anomalous wing-like signal gradually emerges below T_{charge} , whereas the normally behaving, narrower main peak is gradually wiped out [T. Imai et al., Phys. Rev. B **96**, 224508 (2017)]. Furthermore, we show that the enhancement of low energy spin excitations in the low temperature regime below $T_{\text{spin}}^{\text{neutron}} (\simeq T_c)$ depends strongly on the magnitude and orientation of the applied magnetic field.

I. INTRODUCTION

NMR probes the local electronic properties of solids via the hyperfine interactions between the observed nuclear spins and surrounding electrons. If the magnetic hyperfine interactions at a given atomic site are too strong, the NMR linewidth and relaxation rates usually undergo tremendous enhancement as one approaches magnetic instabilities from higher temperatures [1, 2]. For example, ^{63}Cu NMR and NQR (Nuclear Quadrupole Resonance) linewidth and relaxation rates grow exponentially in the paramagnetic state of undoped La_2CuO_4 due to the exponential growth of the spin-spin correlation length ξ [3, 4]. Accordingly, detection of the paramagnetic ^{63}Cu NMR and NQR signals becomes difficult below ~ 400 K, nearly 100 K above the three-dimensional Néel transition at $T_N \simeq 325$ K. This is also the fundamental reason behind the gradual disappearance of ^{63}Cu NMR signals in the charge ordered state of La_2CuO_4 -based cuprates

near the doping concentration around $x \sim 1/8$, because a growing volume fraction of CuO_2 planes have divergently strong spin correlations [5–7].

In La_2CuO_4 , the magnetic hyperfine interactions with Cu electron spins are two orders of magnitude weaker at the ^{139}La (nuclear spin $I = 7/2$ with the nuclear gyromagnetic ratio of $\gamma_n/2\pi = 6.01$ MHz/T) sites than at ^{63}Cu sites: the static hyperfine field B_N arising from Cu spins ordered in a staggered configuration is $B_N \simeq 0.09$ T at ^{139}La sites [8], whereas $B_N \simeq 7.9$ T at ^{63}Cu sites [9], both pointing along the diagonal direction within the CuO_2 plane. Such a modest hyperfine coupling limits the growth of the ^{139}La NMR linewidth and relaxation rates, and hence ^{139}La NMR signals are always observable both above and below T_N [8]. Accordingly, ^{139}La NMR is an effective probe of magnetic instabilities of the CuO_2 planes in the La_2CuO_4 -based superconductors, and played a crucial role in the early days of research into high temperature superconductivity by establishing the

magnetic phase diagram [10–12].

^{139}La NMR was also used extensively to probe the stripe phase [13, 14] of the superconducting $\text{La}_{1.885}\text{Sr}_{0.115}\text{CuO}_4$ ($T_c \simeq 30$ K) and related cuprates from early days [6, 15–21], but the jumble of ^{139}La NMR data acquired for different samples with different measurement conditions did not lead to a coherent physical picture for several reasons: First and foremost, many of the earlier ^{139}La NMR experiments in $\text{La}_{1.885}\text{Sr}_{0.115}\text{CuO}_4$ were limited to low temperature regions without realizing that a charge order transition was lurking at as high as $T_{charge} \simeq 80$ K [22–24]. Second, the lack of single crystals in the early days forced researchers to conduct powder NMR or zero field NQR, and hence only limited information was obtained. Third, as we discussed in great detail in the context of ^{139}La NQR data for the charge and spin ordered $\text{La}_{1.875}\text{Ba}_{0.125}\text{CuO}_4$ and $\text{La}_{1.68}\text{Eu}_{0.2}\text{Sr}_{0.12}\text{CuO}_4$ [6], the glassy nature of spin ordering complicates the interpretation of the NMR data, because the apparent spin ordering temperature depends on the measurement time scales.

For example, in the prototypical stripe ordered materials such as $\text{La}_{1.48}\text{Nd}_{0.4}\text{Sr}_{0.12}\text{CuO}_4$, $\text{La}_{1.68}\text{Eu}_{0.2}\text{Sr}_{0.12}\text{CuO}_4$ and $\text{La}_{1.88}\text{Ba}_{0.12}\text{CuO}_4$ with the low temperature tetragonal (LTT) structure, elastic neutron scattering detects magnetic Bragg peaks at as high as $T_{spin}^{neutron} \simeq 50$ K [13, 25], because of the extremely fast measurement time scales ($\sim 10^{-11}$ s) related to the integral taken over a small but finite energy transfer. On the other hand, μSR measurements, conducted in zero applied magnetic field, require a hyperfine magnetic field to be static over the duration of ~ 0.1 μs to detect the Larmor precessions in a magnetically ordered state, and a spin stripe order appears to occur only below $T_{spin}^{\mu\text{SR}} \simeq 35$ K [14, 26, 27]. The apparent discrepancy arises, simply because fluctuations of Cu moments continue to slow down gradually below $T_{spin}^{neutron}$ rather than suddenly becoming completely static. Our ^{139}La NQR measurements of the nuclear spin $I_z = \pm 3/2$ to $\pm 1/2$ transition at ~ 6 MHz registered the onset of line broadening due to a static B_N at even lower temperatures, ~ 20 K [6]. This is because NMR measurement time scale depends on the NMR frequency and the separation time τ between the 90 and 180 degree radio-frequency pulses, and the latter is generally several μs or longer.

In this paper, we report new high-precision ^{139}La NMR measurements on a $\text{La}_{1.885}\text{Sr}_{0.115}\text{CuO}_4$ single crystal. We independently verified the gradual onset of charge order transition at $T_{charge} \simeq 80$ K by x-ray scattering measurements conducted at the SLAC [24]. We definitively identify the ^{139}La NMR signatures of charge order transition at $T_{charge} \simeq 80$ K, the onset of the three dimensional spin order at $T_{spin}^{neutron} \simeq 30$ K detected at the very fast time scale of elastic neutron scattering measurements, and the onset of spin freezing at the slower time scale of μSR measurements at $T_{spin}^{\mu\text{SR}} \simeq 15 - 20$ K. We unequivocally demonstrate that charge order at $T_{charge} \simeq 80$ K

turns on inhomogeneous growth of low frequency spin fluctuations, in agreement with our earlier conclusions [5–7]. On the other hand, since the amplitude of the charge density modulation is extremely small in the charge ordered state of $\text{La}_{1.885}\text{Sr}_{0.115}\text{CuO}_4$, as is evidenced by the difficulties faced by scatterers to detect Bragg peaks, we found no concrete evidence for a change in the electric field gradient (EFG). Contrary to the presumption made by many authors, however, charge order in $\text{La}_{1.885}\text{Sr}_{0.115}\text{CuO}_4$ sets in very inhomogeneously in space, and a certain volume fraction of the CuO_2 plane is not significantly affected by charge order even below T_{charge} ; such a volume fraction gradually diminishes with decreasing temperature. Furthermore, we show that B_{ext} applied normal to the CuO_2 planes enhances the low frequency spin fluctuations below $T_{spin}^{neutron} (\simeq T_c)$.

II. EXPERIMENTAL

We used a single crystal of $\text{La}_{1.885}\text{Sr}_{0.115}\text{CuO}_4$ grown at Tohoku with the traveling solvent floating zone techniques. The approximate dimensions of the crystal are $2.5 \text{ mm} \times 2.5 \text{ mm} \times 1 \text{ mm}$, and the long edges are parallel with the Cu-O-Cu bond direction. Magnetic susceptibility measurements using a superconducting quantum interference device (SQUID) showed a sharp bulk superconducting transition at $T_c = 30$ K. We used an analogous specimen cut from the same boule of the present crystal for high precision x-ray diffraction experiments at the SLAC, and detected a gradual onset of charge order below $T_{charge} \simeq 80$ K [24]. A similar crystal of the same composition, also grown at Tohoku, was previously shown to exhibit an onset of static spin order at $T_{spin}^{neutron} \simeq T_c \simeq 30$ K [28] at the neutron time scale and $T_{spin}^{\mu\text{SR}} \simeq 20$ K [29] at the μSR time scale.

We conducted all the NMR measurements at McMaster based on standard pulsed NMR techniques using a state-of-the-art NMR spectrometer built around the Redstone NMR console acquired from Tecmag Inc. For the field geometry of $B_{ext} \parallel ab$ -plane, we utilized an aforementioned longer edge of the crystal as a guide for the alignment, and hence the external magnetic field B_{ext} is applied along the Cu-O-Cu bond direction.

We recently used the same piece of crystal for systematic ^{63}Cu NMR measurements above and below T_{charge} for a wide range of NMR pulse separation time from $\tau = 2$ μs to 30 μs [7]. We demonstrated that a relatively narrow central peak with properties analogous to the optimally superconducting $\text{La}_{1.85}\text{Sr}_{0.15}\text{CuO}_4$ is gradually wiped out below T_{charge} , and the missing spectral weight is transferred to an extremely broad, wing-like NMR signal; the latter can be detected only with very short $\tau \lesssim 4$ μs , and exhibits signatures of strongly enhanced spin correlations in the broad lineshape and fast relaxation rates $1/T_1$ and $1/T_2$ [7].

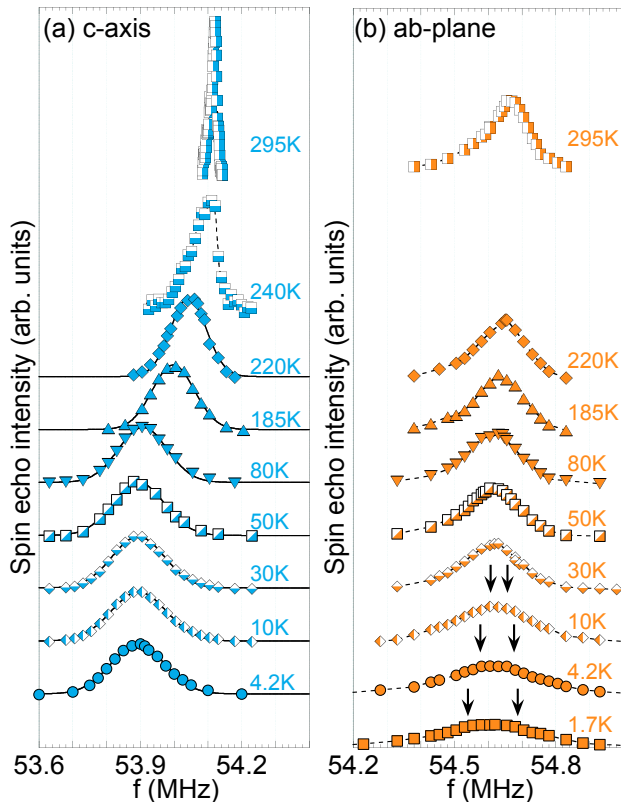


FIG. 1. (a) Representative ^{139}La NMR lineshapes measured with a single crystal in $B_{ext} = 9$ T applied along (a) the c-axis and (b) the Cu-O-Cu bond direction within the ab-plane. For clarity, the vertical origin is shifted at different temperatures. The solid curves through the c-axis results at 220 K and below are the best Gaussian fit, whereas the dashed lines through all other asymmetrical lineshapes are a guide for the eyes. Notice that the lineshape continues to broaden even below $T_{spin}^{neutron} = 30$ K for the ab-plane, and the relatively sharp peak gives way to a wider flat-topped peak with two shoulders below ~ 10 K, as marked by two arrows. Note that the shoulders are hardly observable even at ~ 10 K ($\ll T_{spin}^{neutron}$).

III. RESULTS AND DISCUSSIONS

1. ^{139}La NMR linewidth Δf

In Fig. 1(a), we summarize ^{139}La NMR lineshapes observed for the nuclear spin $I_z = +1/2$ to $-1/2$ central transition in an external magnetic field $B_{ext} = 9$ T applied along the crystal c-axis. We also summarize the peak frequency f_o and the half width at the half maximum (HWHM) of the lineshape Δf in Fig. 2. For this field geometry, the ^{139}La NMR lineshape above $T_{HTT-LTO}$ is so sharp that one can even use Δf to make fine adjustment for the alignment of the crystal [30, 31]. This is because the CuO_6 octahedra point straight up

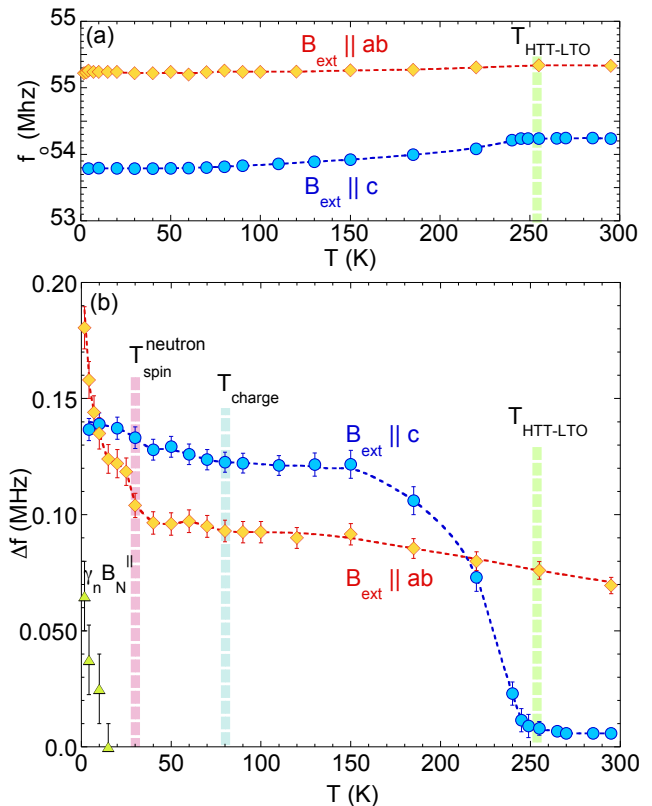


FIG. 2. (a) Temperature dependence of the ^{139}La NMR peak frequency f_o . (b) The HWHM of the ^{139}La NMR lineshape, Δf . Dashed curves are a guide for eyes. Also shown (triangles) are $\gamma_n B_N^{\parallel}$, a half of the split between the two shoulders observed in the ab-plane lineshapes below ~ 10 K in Fig. 1(b), where B_N^{\parallel} is the projection of \vec{B}_N along the direction of the external magnetic field B_{ext} .

along the c-axis, and hence the main principal axis of the electric field gradient (EFG) tensor is parallel with B_{ext} , resulting in null second order quadrupole shift $\Delta\nu_Q^{(2)}$ of f_o . The overall lineshape is asymmetric near 295 K due to the disorder caused by Sr^{2+} substitution, but narrow enough to be captured by the Fast Fourier Transform (FFT) of the spin echo envelope down to 240 K. The half width is as narrow as $\Delta f \simeq 6$ kHz at 295 K.

We found that the lineshape for $B_{ext} \parallel c$ -axis is still somewhat asymmetrical at 220 K, but becomes almost perfect Gaussian at 180 K and below, as shown by solid curves through the lineshapes in Fig. 1(a). Therefore, our results of Δf in Fig. 2(b) have a very high precision below 180 K, the critically important temperature range of our concern in this study. To maintain the consistency with Δf for the symmetrical lineshapes observed below 180 K, we plot Δf estimated from the narrower side of the asymmetric lineshape above 220 K.

As we cross $T_{HTT-LTO} \simeq 250$ K into the LTO structure, the CuO_6 octahedra begin to rotate alternately to-

ward the diagonal direction of the CuO_2 square-lattice [32]. This results in a finite and temperature dependent $\Delta\nu_Q^{(2)} \propto \nu_Q^2/\gamma_n B_{ext}$ even for $B_{ext} \parallel c$, where the nuclear quadrupole frequency at the ^{139}La sites is $\nu_Q \sim 5.5$ MHz. Therefore, the peak frequency f_o shifts lower, as summarized in Fig. 2(a). Since both the rotation angle and ν_Q have a distribution due to the disorder caused by Sr^{2+} substitution, Δf is strongly enhanced by the lattice effects below $T_{HTT-LTO}$, as readily seen in Fig. 1(a) and 2(b).

Let us turn our attention to the magnetic field geometry of $B_{ext} \parallel ab$ -plane. As shown in Fig. 1(b), the lineshape is always asymmetric and already broad at 295 K, because $\Delta\nu_Q^{(2)}$ is sizable for this geometry even in the HTT structure. With decreasing temperature, the NMR line is further broadened by a wide distribution of the rotation angle of the CuO_6 octahedra.

For both the $B_{ext} \parallel c$ -axis and $B_{ext} \parallel ab$ -plane geometries, Δf saturates below ~ 150 K. We confirmed from the measurements at 4.5 T that Δf above T_{charge} is inversely proportional to B_{ext} within experimental uncertainties. This means that Δf is dominated by the structural effects through the distribution of the EFG, because $\Delta\nu_Q^{(2)} \propto 1/B_{ext}$.

As noted above, owing to the nearly perfect Gaussian lineshapes, our estimation of Δf for $B_{ext} \parallel c$ is of very high accuracy below 180 K. At $T_{charge} \simeq 80$ K, Δf begins to show a subtle but clear sign of broadening again. Asymmetrical lineshapes make determination of Δf with equally high precision more difficult for $B_{ext} \parallel ab$, but Δf also grows by a somewhat smaller amount from T_{charge} to ~ 50 K. We confirmed that the increase of Δf below T_{charge} is suppressed by a factor of ~ 2 in 4.5 T. We also confirmed that the splitting ν_Q between the $I_z = +1/2$ to $-1/2$ central peak and the $I_z = \pm 1/2$ to $\pm 3/2$ satellite peaks hardly changes between T_{charge} and 30 K, and the width of the latter remains unchanged across T_{charge} . Accordingly, the observed line broadening in the charge ordered state is paramagnetic in origin, rather than the consequence of nuclear quadrupole effects. This implies that charge density modulation is *not* the direct cause of the broadening of Δf below T_{charge} , presumably because the amplitude of the charge density modulation is very small. Instead, enhanced spin correlations triggered by charge order are the indirect cause of the line broadening observed below T_{charge} . These findings are consistent with the strong paramagnetic ^{63}Cu NMR line broadening we recently reported below T_{charge} for $\tau \sim 2$ μs . [7].

Although almost within experimental uncertainties, Δf seems to reach a plateau below ~ 50 K for both field geometries, before additional line broadening sets in slightly above $T_{spin}^{neutron} \simeq 30$ K. Again, the latter signals additional enhancement of antiferromagnetic spin correlations immediately before three-dimensional spin order begins at $T_{spin}^{neutron}$.

Δf reaches another plateau at ~ 20 K for both $B_{ext} \parallel c$ and $B_{ext} \parallel ab$ geometries, followed by strong enhance-

ment only for $B_{ext} \parallel ab$ below $T_{spin}^{\mu\text{SR}} \simeq 15 \sim 20$ K, where earlier μSR measurements showed that muons begin to exhibit Larmor precession about a static hyperfine magnetic field [14, 29]. Below ~ 10 K, shoulders develop in the lineshapes as shown in Fig. 1(b), which we attribute to the emergence of a static hyperfine magnetic field \vec{B}_N at the ^{139}La sites in the NMR measurement time scale. In what follows, we denote the projection of \vec{B}_N along the direction of \vec{B}_{ext} as B_N^{\parallel} . Depending on the orientation of \vec{B}_N with respect to \vec{B}_{ext} , the static field B_N^{\parallel} either enhances or suppresses the total magnetic field $B_{ext} \pm B_N^{\parallel}$ seen by each ^{139}La nuclear spin, resulting in the upper and lower shoulder in the line shape, respectively. The temperature dependence of $\gamma_n B_N^{\parallel}$ summarized in Fig. 2(b) therefore reflects that of the magnitude of the statically ordered Cu moments in the NMR measurement time scale. The slow growth of B_N observed below ~ 10 K in the present case is in contrast with our earlier finding that B_N quickly saturates in the low temperature tetragonal (LTT) structure of $\text{La}_{1.875}\text{Ba}_{0.125}\text{CuO}_4$ and $\text{La}_{1.68}\text{Eu}_{0.2}\text{Sr}_{0.12}\text{CuO}_4$ below ~ 5 K and ~ 10 K, respectively [6]. We also recall that a transverse magnetic field applied along the CuO_2 planes has been shown to induce a spin flop transition above ~ 5 T in $\text{La}_{1.885}\text{Sr}_{0.115}\text{CuO}_4$ [33, 34] and above ~ 7 T in $\text{La}_{1.875}\text{Ba}_{0.125}\text{CuO}_4$ [20]. Due to the extremely weak NMR signal intensity below T_c for a single crystal sample in the field geometry of $B_{ext} \parallel ab$, the details of the spin-flop transition is beyond the scope of the present work.

We note that the magnitude of B_N^{\parallel} has a large distribution stretching down to zero, and hence the ^{139}La NMR line does not completely split even at 1.7 K. We measured the lineshape at 1.7 K in Fig. 1(b) by repeating the spin echo pulse sequence every $t_{rep} = 23$ ms to saturate the slower component. The central part of the peak with longer T_1 grows if we allow the nuclear spins to fully recover by using longer values of t_{rep} , resulting in somewhat obscured shoulders. The existence of ^{139}La sites with $B_N^{\parallel} \simeq 0$ observed here is consistent with an earlier report that Zeeman perturbed ^{139}La NQR line does not split completely and just broadens [16]. These results are different from a sinusoidally modulating \vec{B}_N expected for a homogeneous incommensurate spin density wave state throughout the entire volume of the sample [35]. μSR measurements also showed that ~ 80 % of the volume fraction of the CuO_2 planes remains paramagnetic even at the base temperature, in which muons do not exhibit Larmor precession [29]; therefore, we should indeed expect that as much as ~ 80 % of ^{139}La sites might continue to see $B_N^{\parallel} \sim 0$ at 1.7 K.

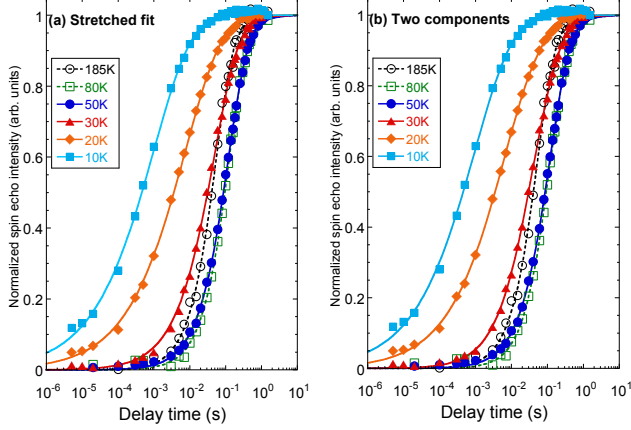


FIG. 3. (a) Representative spin echo recovery curves $M(t)$ after an inversion pulse. At T_{charge} and above, a free parameter fit with Eq. (2) leads to $\beta = 1$ within experimental uncertainties (dashed curves). In the charge ordered state, a growing distribution $1/T_1$ results in $\beta < 1$ (solid curves). See Fig. 4(b) for the temperature dependence of β . (b) Two component fits with Eq. (3), with fast $1/T_1^{fast}$ and slow $1/T_1^{slow}$ components.

2. Volume averaged behavior of low frequency spin dynamics below T_{charge}

In order to investigate the influence of charge and spin order on Cu spin dynamics, we measured the nuclear spin-lattice relaxation rate $1/T_1$ at the central peak of the ^{139}La sites. In the case of ^{63}Cu and ^{17}O NMR experiments, one can probe the different parts of the CuO_2 planes with a different local hole concentration x_{local} by measuring $1/T_1$ at a different frequency within a single NMR peak [31, 36]. In the present case, ^{139}La NMR signals from all different environments are superposed in a single peak, and hence we need to pay careful attention to the volume averaged nature of the ^{139}La $1/T_1$ results when we interpret their implications.

Quite generally, $1/T_1$ probes the Fourier component at the NMR frequency $f_o (= \omega_o/2\pi)$ of the fluctuating hyperfine magnetic fields,

$$\frac{1}{T_1} = \frac{1}{2\hbar^2} \int_{-\infty}^{+\infty} \Sigma_{\alpha} \langle h_{\alpha}(\tau)h_{\alpha}(0) \rangle e^{-i\omega_o\tau} d\tau, \quad (1)$$

where the summation for α is over two directions that are orthogonal to the quantization axis of nuclear spins set by B_{ext} , and h_{α} represents the time dependent fluctuating hyperfine magnetic field along the α axis [1]. If we apply $B_{ext} \parallel c$ to measure $1/T_1$, the quantization axis is along the c -axis, and hence $\alpha = a$ or b . That is, $1/T_1$ measured in $B_{ext} \parallel c$ probes the fluctuating hyperfine fields from Cu spins within the CuO_2 planes, while $1/T_1$ measured in $B_{ext} \parallel ab$ probes the fluctuations along both the c and

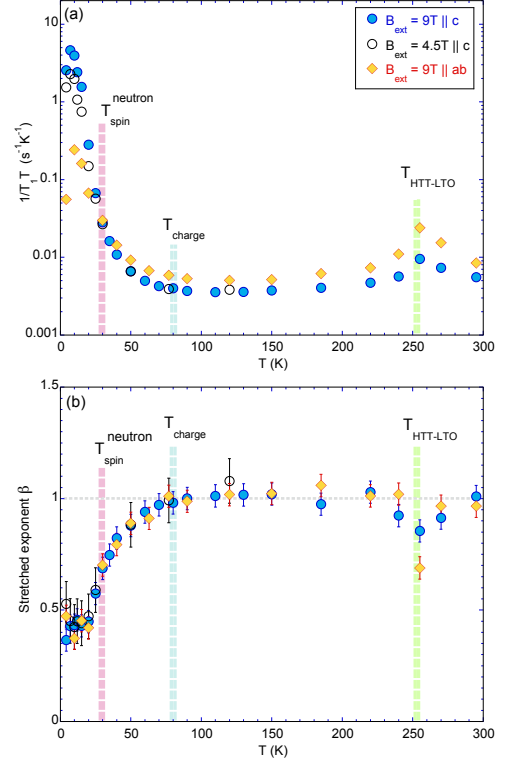


FIG. 4. (a) Temperature dependence of $1/T_1T$ deduced from the best fit with Eq. (2), with a phenomenological stretched exponent β measured in $B_{ext} = 9$ T and 4.5 T applied along the c -axis or ab -planes. (b) Temperature dependence of the stretched exponent β .

ab plane.

In Fig. 3(a), we summarize representative results of the spin echo recovery curve $M(t)$ after an inversion pulse in an external magnetic field 9 T applied along the c -axis. The solid curves represent the best fit with the appropriate fitting function deduced for the magnetic transition ($\Delta I_z = \pm 1$),

$$M(t) = A - B[\Sigma_i p_i \cdot e^{-(q_i t/T_1)^{\beta}}], \quad (2)$$

where A and B are fitting parameters for the saturated and inverted signal intensity, respectively, and the coefficients (p_i, q_i) are theoretically calculated for each relevant normal mode [37, 38]. For clarity, we present the normalized $M(t)$ data in Fig. 3(a), so that it appears to be $A = B = 1$ at all temperatures. β is an additional phenomenological parameter to enable the fit when the relaxation rate $1/T_1$ has a distribution. If the relaxation process is purely magnetic and has no distribution, we expect $\beta = 1$. The stretched exponent β also enables us to fit $M(t)$ phenomenologically, when the additional quadrupolar relaxation process with the $\Delta I_z = \pm 2$ transitions contributes to the relaxation through the fluctuating EFG near the structural phase transition at $T_{HTT-LTO}$ [37, 39]. Separation of the quadrupole con-

tribution to $1/T_1$ is known to be a highly complicated process [39] and beyond the scope of the present work.

In Fig. 4(a), we summarize the temperature dependence of $1/T_1$ divided by T , $1/T_1T$, which reflects the wave vector \mathbf{q} -integral within the first Brillouin zone of the imaginary part of the dynamical electron spin susceptibility $\chi''(\mathbf{q}, f_o)$ at the NMR frequency f_o [40]. As explained in the *Introduction*, the hyperfine field $B_N \sim 0.09$ T is finite at the ^{139}La sites in the Néel state of La_2CuO_4 . By definition, the wave vector \mathbf{q} dependent hyperfine form factor $A_{hf}(\mathbf{q})$ at the ^{139}La sites is related to B_N and the ordered Cu moment μ_{eff} as $B_N = |A_{hf}(\mathbf{q} = \mathbf{Q}_{AF})| \cdot \mu_{eff}$, where $\mathbf{Q}_{AF} = (\pi/a, \pi/a)$. This means that $A_{hf}(\mathbf{q} = \mathbf{Q}_{AF})$ is finite for the staggered wave vector \mathbf{Q}_{AF} , and hence antiferromagnetic spin fluctuations near $\mathbf{q} \sim \mathbf{Q}$ can contribute to $1/T_1$ measured at the ^{139}La sites.

Summarized in Fig. 4(b) is the temperature dependence of the corresponding stretched exponent β . $1/T_1T$ shows very little temperature dependence down to T_{charge} except for a small cusp at $T_{HTT-LTO}$ due to the enhanced slow fluctuations of the EFG associated with the lattice vibrations slowing down toward the structural transition [41]. The stretched exponent also deviates from $\beta = 1$ near $T_{HTT-LTO}$, because the contribution of the additional quadrupole relaxation process invalidates the underlying assumption for the derivation of Eq. (2) based on purely magnetic transitions.

Once charge order sets in at $T_{charge} \simeq 80$ K, two qualitative changes take place. First, as shown in Fig. 4(a), $1/T_1T$ begins to grow dramatically. Analogous enhancement of $1/T_1T$ takes place below T_{charge} also at the planar ^{17}O sites [18, 42]. These findings indicate that low frequency Cu spin fluctuations averaged over the entire volume of the sample undergo a dramatic enhancement in the charge ordered state as temperature is lowered toward the onset of spin order at $T_{spin}^{neutron} \simeq 30$ K. We cannot entirely rule out a possibility from this data alone that quadrupole relaxation through fluctuating EFG is enhanced in the charge ordered state. However, we believe such a scenario is unlikely, because anomalous wing-like signals emerge for ^{63}Cu NMR below T_{charge} with signatures of enhanced spin correlations [7]. Inelastic neutron scattering experiments conducted with low energy transfer also evidenced that low frequency spin fluctuations are enhanced below T_{charge} [43].

Unlike the typical second order magnetic phase transitions, $1/T_1T$ does not diverge at $T_{spin}^{neutron} \simeq 30$ K. That is, critical slowing down of spin fluctuations does not lead to divergently large $\chi''(\mathbf{Q}, f_o)$ at $T_{spin}^{neutron}$ (\mathbf{Q} represents the ordering wave vector reported in [28]). Instead, $1/T_1T$ keeps growing through $T_{spin}^{neutron}$, and exhibits a broad hump centered around ~ 8 K. In other words, spin ordering is indeed glassy, and the fluctuation time scale of Cu spins continue to slow down through $T_{spin}^{neutron} \simeq 30$ K and $T_{spin}^{\mu SR} \simeq 20$ K; the average fluctuation frequency finally slows down to f_o only at ~ 8 K. This finding is consistent with the fact that the static hyperfine magnetic

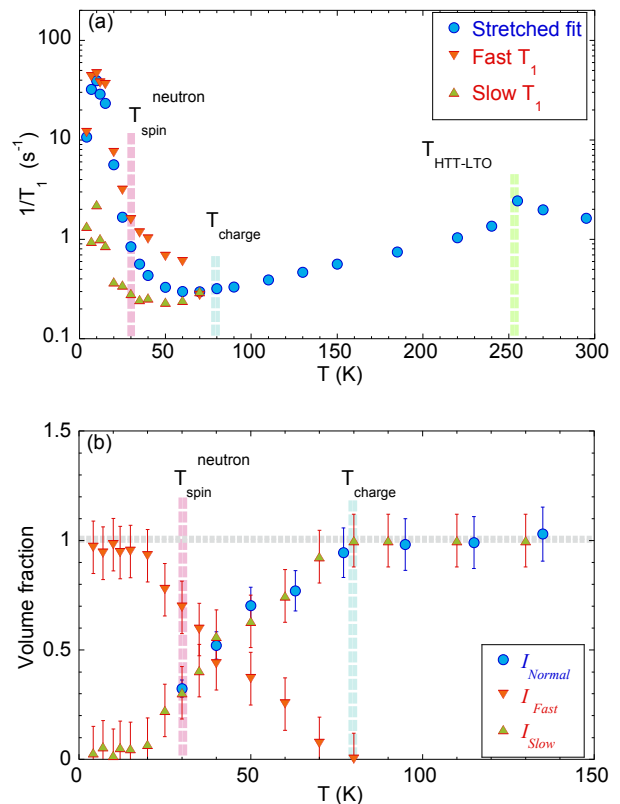


FIG. 5. (a) Comparison of $1/T_1$ for $B_{ext} \parallel c$ deduced from the stretched fit with Eq. (2) (filled bullets; also shown in Fig. 4(a) in the form of $1/T_1T$ rather than $1/T_1$) vs. two $1/T_1^{fast}$ and $1/T_1^{slow}$ values deduced from the two component fit with Eq. (3) (downward and upward triangles). (b) The fraction of ^{139}La nuclear spins involved in the slower $1/T_1$ component (upward triangles) show identical behavior as the spectral weight I_{Normal} of the narrower, normally behaving ^{63}Cu NMR peak that seems almost oblivious to charge order and gradually wiped out below T_{charge} (adopted from Imai et al. [7]).

field B_N begins to grow gradually below $T_{spin}^{\mu SR} \simeq 20$ K.

The second change that manifests itself below T_{charge} is that the phenomenological stretched exponent begins to deviate from $\beta = 1$. This implies that the magnitude of $1/T_1$ develops a broad range of distribution starting from T_{charge} toward the glassy spin ordering below $T_{spin}^{neutron}$.

3. Two component behavior of low frequency spin dynamics below T_{charge}

The phenomenological stretched fit with $\beta < 1$ presented in Fig. 3(a) is satisfactory, but one needs to be cautious in interpreting the resulting value of $1/T_1$ because of its broad distribution. In fact, closer examination of the recovery curves observed at 30 K and 185 K

in Fig. 3(a) reveals that the former crosses the latter. That is, the distributed $1/T_1$ at 30 K has both faster and slower components than a single valued $1/T_1$ at 185 K. Our observation that a significant fraction of ^{139}La nuclear spins still relax slowly below T_{charge} corroborates with our recent finding that two different types of ^{63}Cu NMR signals exist below T_{charge} , as mentioned at the end of section II: the spectral weight I_{Normal} of the normally behaving narrow ^{63}Cu NMR peak with slower $1/T_1$ is gradually wiped out below T_{charge} , as reproduced from [7] in Fig. 5(b). The lost spectral weight is transferred to an anomalously broad, wing-like ^{63}Cu NMR signal which exhibit extremely fast $1/T_1$.

Since NMR is a local probe, if ^{63}Cu NMR signals behave completely differently in a certain volume fraction, I_{Normal} , of the the CuO_2 planes, ^{139}La NMR properties in the same volume would also be completely different. Accordingly, to maintain consistency between the ^{139}La and ^{63}Cu NMR results, it makes more sense to fit the recovery curves $M(t)$ with two components,

$$M(t) = A - B_1[\sum_i p_i \cdot e^{-(q_i t/T_1^{fast})^\beta}] - B_2[\sum_i p_i \cdot e^{-(q_i t/T_1^{slow})}]. \quad (3)$$

To achieve a good fit, we kept the stretched exponent β for the faster component $1/T_1^{fast}$, which arises from the segments of the CuO_2 plane that yield the anomalous wing-like ^{63}Cu NMR signal with extremely fast $1/T_1$; the slower component $1/T_1^{slow}$ arises from the normally behaving volume in which ^{63}Cu NMR properties seem almost oblivious to charge order even below T_{charge} . As shown in Fig. 3(b), the alternate fits with Eq. 3 are equally good.

We compare $1/T_1^{fast}$ and $1/T_1^{slow}$ in Fig. 5(a). The temperature dependence of β for the two component fit is very similar to the result in Fig. 4(b). The behavior of $1/T_1^{fast}$ is very similar to the volume averaged $1/T_1$ estimated from the stretched fit using Eq. 2. $1/T_1^{slow}$, however, continues to decrease from T_{charge} down to the onset of spin order at $T_{spin}^{neutron}$. The observed temperature dependence of $1/T_1^{slow}$ is qualitatively similar to the temperature dependence observed for the optimally superconducting $\text{La}_{1.85}\text{Sr}_{0.15}\text{CuO}_4$ above its $T_c = 38$ K [44, 45].

Summarized in Fig. 5(b) is the volume fractions $I_{slow} = B_2/(B_1 + B_2)$ and $I_{fast} = B_1/(B_1 + B_2) = 1 - I_{slow}$ in which ^{139}La nuclear spins relax with $1/T_1^{slow}$ and $1/T_1^{fast}$, respectively. Quite remarkably, I_{slow} shows identical behavior as I_{Normal} , as expected, and gradually diminishes below T_{charge} . In contrast, I_{fast} grows from 0 % at T_{charge} to ~ 70 % at $T_{spin}^{neutron} \simeq T_c \simeq 30$ K, then to nearly 100 %. The fact that I_{fast} reaches ~ 100 % at ~ 20 K seems to suggest that, although the μSR data showed ~ 80 % of the sample volume remains paramagnetic without a static hyperfine field [29], the entire volume of the CuO_2 planes are in fact under the influence of enhanced spin fluctuations below ~ 20 K. A potential caveat for this argument is that, since the superconducting shielding effects limit the NMR signal intensity below

$T_{spin}^{neutron} \simeq T_c \simeq 30$ K, we may be probing mostly the magnetic volume rather than the superconducting volume. But such a scenario seems highly unlikely in view of the fact that I_{slow} smoothly decreases through T_c .

4. Magnetic field effects on low energy spin excitations

Earlier elastic neutron scattering experiments found that application of a magnetic field normal to the CuO_2 planes enhances the magnetic Bragg peak intensity arising from ordered spins below $T_{spin}^{neutron}$ [46, 47]. Such enhancement has been often attributed to the field-induced ordered moments within the superconducting vortex cores. In Fig. 4(a), we compare $1/T_1T$ measured in a magnetic field $B_{ext} = 9$ T and 4.5 T applied along the c -axis. The $1/T_1T$ results show no field dependence down to $T_c \simeq T_{spin}^{neutron} \simeq 30$ K, where a substantial field dependence sets in. Interestingly, $1/T_1T$ reaches the maximum at the same temperature ~ 8 K for 9 T and 4.5 T, but the peak magnitude of $1/T_1T$ in 9 T is almost exactly twice larger than that observed in 4.5 T. Our finding is certainly consistent with the popular interpretation of the neutron data; when we apply twice stronger B_{ext} , the volume encompassed in the vortex core is doubled and hence its fast contribution to the volume averaged $1/T_1T$ also doubles. Note, however, that such an argument is based on an assumption that both superconductivity and magnetic order take place uniformly within the CuO_2 planes, which may not be necessarily the case in $\text{La}_{1.885}\text{Sr}_{0.115}\text{CuO}_4$ according to local probe measurements reported here and elsewhere [5, 7, 29].

Another interesting aspect of our results in Fig. 4(a) is the anisotropy of $1/T_1$. The faster growth of $1/T_1T$ observed somewhat below T_{charge} for the $B_{ext} \parallel c$ than $B_{ext} \parallel ab$ geometry indicates that low frequency spin fluctuations are more strongly enhanced within the ab -plane. This is consistent with the fact that Cu spins eventually order along the CuO_2 planes in the low temperature limit, as evidenced by the static hyperfine field \vec{B}_N pointing along the CuO_2 planes.

Below ~ 15 K, the anisotropy of $1/T_1T$ reaches a factor of ~ 10 . An interesting possibility is that this is also caused by superconducting vortices. In $B_{ext} = 9$ T $\parallel ab$, the applied field is much smaller than the superconducting critical field B_{c2} owing to the layered structure, and the superconducting coherence length ξ is highly anisotropic ($\xi_c \ll \xi_{ab}$). The area encompassed in the vortex core $\sim \pi\xi_{ab}\xi_c$ for $B_{ext} \parallel ab$ is much smaller than $\sim \pi\xi_{ab}^2$ for $B_{ext} \parallel c$. Therefore, much smaller peak value of $1/T_1T$ for $B_{ext} = 9$ T $\parallel ab$ may be a consequence of the weaker influence of vortex cores penetrating through the CuO_2 planes. (The extremely small $1/T_1T \sim 0.5$ s $^{-1}$ K $^{-1}$ observed at 4.2 K for $B_{ext} = 9$ T $\parallel ab$ may be caused by the fact that we measured $1/T_1$ at the center of the peak, where B_N^{\parallel} is vanishingly small.)

IV. SUMMARY AND CONCLUSIONS

Three decades have passed since the discovery of high T_c superconductivity in La_2CuO_4 -based materials, yet many fundamental issues remain unsolved. ^{139}La NMR in high magnetic fields is among the most straightforward NMR experiments for cuprates in terms of the technical requirements. Nonetheless, there was no comprehensive single crystal ^{139}La NMR work on charge and spin ordered high T_c superconductor $\text{La}_{1.885}\text{Sr}_{0.115}\text{CuO}_4$ to date. Moreover, the physics of this composition has long been controversial, in part because glassiness of spin order and existence of superconductivity in spin ordered CuO_2 planes complicate the interpretation of experimental results. The controversy also stemmed from the fact that charge order Bragg peaks could not be detected by diffraction experiments until recently, and hence many researchers had continued to argue against the presence of charge order. We emphasize that we concluded the presence of charge order in $\text{La}_{1.885}\text{Sr}_{0.115}\text{CuO}_4$ with or without Eu co-doping [5, 6, 48], $\text{La}_{1.875}\text{Ba}_{0.125}\text{CuO}_4$ [5, 6, 48], and $\text{La}_2\text{CuO}_{4+y}$ [49] in as early as 1999, based on our findings that peculiar NMR anomalies associated with charge order of $\text{La}_{1.48}\text{Nd}_{0.4}\text{Sr}_{0.12}\text{CuO}_4$ are shared by all of these materials.

To fill the knowledge gap and provide complementary information to the peculiar two component behavior of ^{63}Cu NMR [5] recently confirmed below T_{charge} [7], we have conducted comprehensive single crystal ^{139}La NMR experiments. From the high precision measurements of the linewidth Δf and spin-lattice relaxation rate $1/T_1$, we have identified the anomalies associated with charge order and glassy spin order, and cleared up the confusions from the past. Combined with the successful detection of charge order Bragg peaks in $\text{La}_{1.885}\text{Sr}_{0.115}\text{CuO}_4$ [22–24] and related materials [25, 50] in recent years, we believe that a clear-cut physical picture is finally emerging.

Perhaps the most significant message from our local probe study, with possibly far reaching implications, is that charge ordered CuO_2 planes in $\text{La}_{1.885}\text{Sr}_{0.115}\text{CuO}_4$ become extremely inhomogeneous, and have two distinct regions with contrasting characteristics: (a) Normal regions with the volume fraction $I_{slow} (\simeq I_{Normal}$ observed for ^{63}Cu NMR [7]), which are not affected significantly by charge order, and (b) charge ordered regions with continuously growing spin correlations from T_{charge} through $T_{spin}^{neutron}$. The ^{139}La and ^{63}Cu NMR properties in the normal regions are qualitatively similar to those observed

for the optimally superconducting $\text{La}_{1.85}\text{Sr}_{0.15}\text{CuO}_4$, but its volume fraction gradually decreases from 100 % at T_{charge} to ~ 0 % at ~ 20 K. It remains to be seen whether our finding is directly related to the nematicity expected for the charge ordered CuO_2 planes [51]. We emphasize that NMR is a local probe. In contrast, neutron and x-ray scattering measurements on charge and spin order phenomena are conducted in the \mathbf{q} -space by integrating the scattering intensity from the entire volume of the sample, and hence probe only the volume averaged behavior of the CuO_2 planes.

We should note that our Δf results for $B_{ext} \parallel ab$ are similar to the pioneering powder ^{139}La NMR data reported by Goto et al. below 60 K [15, 17, 34]. They did not extend their Δf measurements to the crucial temperature region across T_{charge} , because their initial 1994 work preceded the discovery of charge order phenomenon in $\text{La}_{1.48}\text{Nd}_{0.4}\text{Sr}_{0.12}\text{CuO}_4$ by Tranquada et al. in 1995 [13]. More recently, after we concluded that $\text{La}_{1.885}\text{Sr}_{0.115}\text{CuO}_4$ with or without Eu co-doping also undergoes a charge order [5, 6, 18, 48], the Grenoble group reported a limited set of ^{139}La single crystal NMR data for $\text{La}_{1.88}\text{Sr}_{0.12}\text{CuO}_4$ in a tilted magnetic field up to 100 K [19]. Some parts of their results are similar to Goto's results and ours reported here and elsewhere [18]. The Grenoble paper as well as an earlier work on $\text{La}_{1.65}\text{Eu}_{0.2}\text{Sr}_{0.15}\text{CuO}_4$ by the Los Alamos group [52], however, interpreted their NMR data based on a presumption that charge order is absent in the superconducting cuprates. Very recent ^{139}La NMR work on the charge ordered state realized in the LTT structure of $\text{La}_{1.88}\text{Ba}_{0.12}\text{CuO}_4$ with suppressed superconductivity [20] share many similarities with the present case, but there are two important dissimilarities: First, the magnetic correlations in $\text{La}_{1.88}\text{Ba}_{0.12}\text{CuO}_4$ grow very quickly below $T_{charge} = 54$ K, and $1/T_1$ seems to reach a plateau at $T_{spin}^{neutron} = 40$ K. Second, application of a high magnetic field *suppresses* $1/T_1$ in the spin ordered phase of $\text{La}_{1.88}\text{Ba}_{0.12}\text{CuO}_4$, whereas a magnetic field *enhances* $1/T_1$ in the present case.

V. ACKNOWLEDGEMENT

The work at McMaster was financially supported by NSERC and CIFAR. The work at Stanford was supported by US Department of Energy, Office of Science, Office of Basic Energy Sciences under grant no. DE-FG02-07ER46134. The work at Tohoku was supported by Grant-in-Aid for Scientific Research (A) (16H02125).

[1] V. Jaccarino, *Nuclear Resonance in Antiferromagnets*, edited by G. T. Rado and H. Suhl, Vol. Magnetism IIA (Academic Press, 1965).
 [2] P. Heller and G. B. Benedek, Phys. Rev. Lett. **8**, 428 (1962).

[3] T. Imai, C. P. Slichter, K. Yoshimura, and K. Kosuge, Phys. Rev. Lett. **70**, 1002 (1993).
 [4] T. Imai, C. P. Slichter, K. Yoshimura, M. Katoh, and K. Kosuge, Phys. Rev. Lett. **71**, 1254 (1993).

- [5] A. W. Hunt, P. M. Singer, K. R. Thurber, and T. Imai, *Phys. Rev. Lett.* **82**, 4300 (1999).
- [6] A. W. Hunt, P. M. Singer, A. F. Cederström, and T. Imai, *Phys. Rev. B* **64**, 134525 (2001).
- [7] T. Imai, S. K. Takahashi, A. Arsenault, A. W. Acton, D. Lee, W. He, Y. S. Lee, and M. Fujita, *Phys. Rev. B* **96**, 224508 (2017).
- [8] H. Nishihara, H. Yasuoka, T. Shimizu, T. Tsuda, T. Imai, S. Sasaki, S. Kanbe, K. Kishio, K. Kitazawa, and K. Fueki, *J. Phys. Soc. Jpn.* **56**, 4559 (1987).
- [9] T. Tsuda, T. Shimizu, H. Yasuoka, K. Kishio, and K. Kitazawa, *J. Phys. Soc. Jpn.* **57**, 2908 (1988).
- [10] I. Wataneba, K. Kumagai, Y. Nakamura, T. Kimura, Y. Nakamichi, and H. Nakajima, *J. Phys. Soc. Jpn.* **56**, 3028 (1987).
- [11] Y. Kitaoka, K. Ishida, S. Hiramatsu, and K. Asayama, *J. Phys. Soc. Jpn.* **57**, 734 (1988).
- [12] F. C. Chou, F. Borsa, J. H. Cho, D. C. Johnston, A. Lascialfari, D. R. Torgeson, and J. Ziolo, *Phys. Rev. Lett.* **71**, 2323 (1993).
- [13] J. M. Tranquada, B. J. Sternlieb, J. D. Axe, Y. Nakamura, and S. Uchida, *Nature* **375**, 561 (1995).
- [14] K. Kumagai, K. Kawano, I. Watanabe, K. Nishiyama, and K. Nagamine, *Hyperfine Interactions* **86**, 473 (1994).
- [15] T. Goto, S. Kazama, K. Miyagawa, and T. Fukase, *J. Phys. Soc. Jpn.* **63**, 3494 (1994).
- [16] S. Ohsugi, Y. Kitaoka, H. Yamanaka, K. Ishida, and K. Asayama, *J. Phys. Soc. Jpn.* **63**, 2057 (1994).
- [17] T. Goto, T. Suzuki, K. Chiba, T. Shinoda, M. Mori, and T. Fukase, *Physica B* **246-247**, 572 (1998).
- [18] T. Imai and K. Hirota, Unpublished ^{63}Cu , ^{139}La , and ^{17}O NMR work on a $\text{La}_{1.885}\text{Sr}_{0.115}\text{CuO}_4$ single crystal presented first at the Aspen Winter Conference on Quantum Criticality (January 1999).
- [19] V. F. Mitrović, M.-H. Julien, C. de Vaulx, M. Horvatić, C. Berthier, T. Suzuki, and K. Yamada, *Phys. Rev. B* **78**, 014504 (2008).
- [20] S.-H. Baek, Y. Utz, M. Hücker, G. D. Gu, B. Büchner, and H.-J. Grafe, *Phys. Rev. B* **92**, 155144 (2015).
- [21] S.-H. Baek, A. Erb, and B. Büchner, *Phys. Rev. B* **96**, 094519 (2017).
- [22] T. P. Croft, C. Lester, M. S. Senn, A. Bombardi, and S. M. Hayden, *Phys. Rev. B* **89**, 224513 (2014).
- [23] V. Thampy, M. P. M. Dean, N. B. Christensen, L. Steinke, Z. Islam, M. Oda, M. Ido, N. Momono, S. B. Wilkins, and J. P. Hill, *Phys. Rev. B* **90**, 100510 (2014).
- [24] W. He, Y. S. Lee, and M. Fujita, (2017), unpublished.
- [25] M. Fujita, H. Goka, K. Yamada, J. M. Tranquada, and L. P. Regnault, *Phys. Rev. B* **70**, 104517 (2004).
- [26] G. M. Luke, L. P. Le, B. J. Sternlieb, W. D. Wu, Y. J. Uemura, J. H. Brewer, and Riseman, *Physica C* **185-189**, 1175 (1991).
- [27] B. Nachumi, Y. Fudamoto, A. Keren, K. M. Kojima, M. Larkin, G. M. Luke, J. Merrin, O. Tchernyshyov, Y. J. Uemura, N. Ichikawa, M. Goto, H. Takagi, S. Uchida, M. K. Crawford, E. M. McCarron, D. E. MacLaughlin, and R. H. Heffner, *Phys. Rev. B* **58**, 8760 (1998).
- [28] H. Kimura, K. Hirota, H. Matsushita, K. Yamada, Y. Endoh, S.-H. Lee, C. F. Majkrzak, R. Erwin, G. Shirane, M. Greven, Y. S. Lee, M. A. Kastner, and R. J. Birgeneau, *Phys. Rev. B* **59**, 6517 (1999).
- [29] A. T. Savici, Y. Fudamoto, I. M. Gat, T. Ito, M. I. Larkin, Y. J. Uemura, G. M. Luke, K. M. Kojima, Y. S. Lee, M. A. Kastner, R. J. Birgeneau, and K. Yamada, *Phys. Rev. B* **66**, 014524 (2002).
- [30] K. R. Thurber, A. W. Hunt, T. Imai, F. C. Chou, and Y. S. Lee, *Phys. Rev. Lett.* **79**, 171 (1997).
- [31] P. M. Singer, T. Imai, F. C. Chou, K. Hirota, M. Takaba, T. Kakeshita, H. Eisaki, and S. Uchida, *Phys. Rev. B* **72**, 014537 (2005).
- [32] v. B. Grande, H. Mueller-Bushbaum, and M. Schweizer, *Z. Anorg. Allg. Chem.* **428**, 120 (1977).
- [33] T. Goto, K. Chiba, M. Mori, K. Suzuki, t. amd Seki, and T. Fukase, *J. Phys. Soc. Jpn.* **66**, 2870 (1997).
- [34] K. Chiba, T. Goto, M. Mori, T. Suzuki, K. Seki, and T. Fukase, *J. Low Temp. Phys.* **117**, 479 (1999).
- [35] F. L. Ning, M. Fu, D. A. Torchetti, T. Imai, A. S. Sefat, P. Cheng, B. Shen, and H.-H. Wen, *Phys. Rev. B* **89**, 214511 (2014).
- [36] P. M. Singer, A. W. Hunt, and T. Imai, *Phys. Rev. Lett.* **88**, 047602 (2002).
- [37] E. R. Andrew and D. P. Tunstall, *Proceedings of the Physical Society* **78**, A1 (1960).
- [38] A. Narath, *Phys. Rev.* **162**, 320 (1967).
- [39] A. Suter, M. Mali, J. Roos, and D. Brinkmann, *J. Phys.: Condens. Matter* **10**, 5977 (1998).
- [40] T. Moriya, *J. Phys. Soc. Jpn.* **18**, 516 (1963).
- [41] R. J. Birgeneau, C. Y. Chen, D. R. Gabbe, H. P. Jenssen, M. A. Kastner, C. J. Peters, P. J. Picone, T. Thio, T. R. Thurston, H. L. Tuller, J. D. Axe, P. Böni, and G. Shirane, *Phys. Rev. Lett.* **59**, 1329 (1987).
- [42] T. Imai and Y. S. Lee, Accepted for publication in *J. Phys. Soc. Jpn.* (arXiv:1712.09380) (2018).
- [43] A. T. Rømer, J. Chang, N. B. Christensen, B. M. Andersen, K. Lefmann, L. Mähler, J. Gavilano, R. Gildardi, C. Niedermayer, H. M. Rønnow, A. Schneidewind, P. Link, M. Oda, M. Ido, N. Momono, and J. Mesot, *Phys. Rev. B* **87**, 144513 (2013).
- [44] T. Kobayashi, S. Wada, Y. Kitaoka, and K. Asayama, *J. Phys. Soc. Jpn.* **58**, 2262 (1989).
- [45] K. Yoshimura, T. Uemura, M. Kato, T. Shibata, K. Kosuge, T. Imai, and H. Yasuoka, *Springer Proceedings in Physics* **60**, 405 (1992).
- [46] B. Lake, H. M. Ronnow, N. B. Christensen, G. Aeppli, K. Lefmann, D. F. McMorrow, P. Vorderwisch, P. Smeibid, N. Mangkorntong, T. Sasagawa, M. Nohara, H. Takagi, and T. E. Mason, *Nature* **415**, 299 (2002).
- [47] B. Khaykovich, S. Wakimoto, R. J. Birgeneau, M. A. Kastner, Y. S. Lee, P. Smeibid, P. Vorderwisch, and K. Yamada, *Phys. Rev. B* **71**, 220508 (2005).
- [48] P. M. Singer, A. W. Hunt, A. F. Cederström, and T. Imai, *Phys. Rev. B* **60**, 15345 (1999).
- [49] T. Imai and Y. S. Lee, arXiv:1712.09720.
- [50] J. Fink, V. Soltwisch, J. Geck, E. Schierle, E. Weschke, and B. Büchner, *Phys. Rev. B* **83**, 092503 (2011).
- [51] S. A. Kivelson, E. Fradkin, and V. J. Emery, *Nature* **393**, 550 (1998).
- [52] N. J. Curro, P. C. Hammel, B. J. Suh, M. Hücker, B. Büchner, U. Ammerahl, and A. Revcolevschi, *Phys. Rev. Lett.* **85**, 642 (2000).